HEAT TRANSFER ENHANCEMENT USING NON-EQUALLY STRUCTURE IN A PLATE-FIN HEAT EXCHANGER WITH OFFSET FINS

by

***Juan DU*[a*] *and Jun DENG*[b]**

[a] School of Mathematics and Statistics, Fuyang Normal University, Fuyang, Anhui, China
[b] School of Machinery and Automation, Wuhan University of Science and Technology, Hubei, China

Original scientific paper
https://doi.org/10.2298/TSCI211227036D

In this study, a cross-flow plate-fin heat exchanger with offset fins is optimized by considering the effects of flow maldistribution for air side. For this purpose, the study is focused on an increase in the rate of heat transfer, which can be achieved by using non-equally fin structure. Numerical simulations have been carried out to investigate the thermodynamic characteristics of the non-equally full-size plate-fin heat exchanger by using the porous media approach. Based on the numerical model, flow distribution, total heat rate and pressure drop of the plate-fin heat exchanger are studied. A asymmetric structure with heat transfer enhancement is presented in this study. After comparing numerical predictions of the total heat transfer rate and the pressure drop under various Reynolds number. It is observed that, the percentages of increase in effectiveness for the final non-equally structure are in the range of 2.5-6.2% and the pressure drop remains almost constant in the cases of air inlet velocity fixed at 9.5627 m/s. The increasing asymmetric structure is numerically verified to improve the flow distribution of the plate-fin heat exchanger.

Key words: *porous media, CFD, numerical simulation, heat exchanger, non-equally fins*

Introduction

Plate-fin heat exchanger (PFHE) performance with offset fins is of great importance known for their compactness and higher thermal efficiency is widely applied in energy transfer related industrial applications. In the liquid-to-gas and phase-change heat exchangers, the air-side thermal resistance contributes heavily to the overall thermal resistance and liquid with lower thermal resistance through the channels. In the design of PFHE, especially the air side fins, it is generally assumed that the oil-side temperature and flow distribution are uniform. However, the assumption is generally not realistic in the real conditions. The main reason is due to the flow misdistribution. To assess the resultant change in its flow distribution and thermal performance, fins of special shapes on the plates generate high turbulent flow in the flow channels formed by the plates,which enables achievement of heat transfer enhancement. Reduction in air-side thermal resistance gives an increase in the rate of heat transfer, which can be achieved by the structural design of the fins. Number of parallel fins are used to construct the heat exchangers by enhancing the heat transfer surfaces. Over the last few decades, a various of fin patterns have been proposed and their effects has been studied either experimentally or

* Corresponding author, e-mail:dujuan826@163.com

numerically. The vortex generators have shown great promise in enhancing air-side heat transfer coefficient [1-4], where Hemant and Tiwari [5, 6] carried out a series of experimental and numerical investigation of air-flow on the PFHE by winglet type vortex generators. Anupam *et al.* [7] analyzed the flow structure and simulated the air-flow through fin-tube type heat exchangers with rectangular winglet pairs. In recent years, with the development of CFD simulation technology, the details of the internal flow heat transfer and flow distribution can be more intuitively tested and various optimal designs can be determined at a relatively low cost. More recently, citations have studied the thermodynamic characteristics of the PFHE by applying CFD technique. However, due to the increasingly widespread applications of the PFHE, the volume is increasing and the structure becomes more complicated. Therefore, the simulation of full-size heat exchanger needs more computer resources and computing time. So far, no study has yet been carried out to simulate a full-size PFHE by considering the actual number of fins inside the PFHE. This can be accomplished by treating the heat exchanger as porous media model with volume averaged properties. The earliest study of heat exchangers using the porous media was conceptualized by Patankar and Spalding [8] in the so-called distributed-resistance method, which applied to both transient and steady-state analyses of a shell-and-tube heat exchanger, it has been successfully employed in a variety of applications [9-13]. The flow and heat transfer characteristics through the assumption of porous media are approximately identical to the practical test ones, so as to achieve the purpose of the simulation study on the overall structure. Based on this theory, Wang *et al*. [14] applied the porous media solver method to the PFHE with flat fins and the numerical research on the internal fluid is presented. Musto *et al*. [15] used a porous media model to simulate the main effects of the heat exchanger, such as pressure drop and heat rejection, occurred in an aircraft oil cooler system. The investigation of Li *et al.* [16] investigated a single 3-D finned-tube and tube bundles. The numerical verification is conducted on the porous media model based on the cylindrical co-ordinate.

Meanwhile, in the design of the heat exchanger, especially the compact heat exchanger, it is generally assumed that the inlet temperature and flow distribution are uniform [17, 18]. However, the assumption is generally not realistic in the real conditions because of the flow maldistribution and non-uniformity. In order to examine the effects of flow maldistribution in heat exchangers, various configurations of distributors were used with a PFHE under different operation conditions by Zhang *et al.* [19] and the results showed that improved distributors were very effective in improving the flow distribution and thermal performance in heat exchanger. The authors [20-22] used 3-D CFD simulations to predict the impact effect of inlet air-flow maldistribution on thermal-hydraulic performance. Muller-Menzel and Hecht [23] theoretically discussed the occurrence of various flow patterns in a PFHE and their impact on the overall performance of the heat exchanger. Wang *et al.* [14] proposed that header-based strategy and fin channel-based strategy can greatly improve flow distribution of the PFHE, while at the cost of an associated increase in pressure drop, resulting in an extra pumping power. An experimental investigation had been carried out by Rao and Das. [10] to find the flow and the pressure difference across the port to channel in plate heat exchangers for a wide range of Reynolds numbers. The results indicated that the flow maldistribution increased with increasing overall pressure drop. In addition, an optimized model is proposed based on multi objective optimization algorithm by Hajabdollahi and Seifoori [24] considering the effects of flow maldistribution for both cold and hot sides. In the study the effects of air-flow non-uniformity on the thermal-hydraulic performance a fin-and-tube heat exchanger were investigated experimentally. The study found that the non-uniformity of air-flow caused thermal effectiveness deterioration and increasing pressure drop [25]. Ranganayakulu and Seetharamu [26] analyzed the combined effect of longitudinal heat conduction and flow non-uniformity on a crossflow PFHE based on the finite-element method.

In this paper, a cross-flow PFHE, which the oil side is trapezoidal and the air side is rectangular offset strip fins, fig. 1, is modelled and optimized using the non-equally structure including the total heat transfer rate and the pressure drop. Numerical simulations have been carried out to investigate the thermodynamic characteristics of the non-equally full-size PFHE by using the porous media approach. These results are compared with the constant or uniform profile. To generalize the optimum results, the optimization is performed for different hot and cold side mass-flow rates and the results are reported.

The Non-equally structure model

In this study, on the basis of literature [27], the structure was modified and the fins of heat exchanger are gradually increased from the inlet to the adjacent fins on both sides. The arithmetic sequence is arranged and the shape of the oil-side fins remains unchanged to improve the heat transfer effect of the PFHE as is shown in fig. 1.

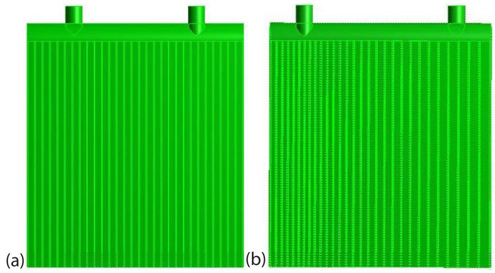

Figure 1. The structure of the PFHE; (a) equally spaced fins and (b) non-equally spaced fins

Numerical simulation

Geometry of solution domain

Figure 2 shows the geometry depiction of the solution domain, which is divided into three areas: the heater area, the distribution area, and the heat transfer area. It has been performed by an air/oil offset plat-fin aluminum heat exchanger with counter current cross-flow, in which air-flow has one channel and oil flow has two passed. Cold air was used to cool hot oil during the whole heat transfer process. To minimize heat loss, the air side was set to 30 layers and the oil side is 29 layers. All components were connected well by brazing welding. Each fin layer was separated by a clapboard to form two different flow channels. The oil-side fins were arranged as trapezoidal staggered to form a *U*-type flow channel. The middle of each layer was separated by the layered seals. Heat transfer area was filled with offset fins. The fluid firstly flows through the inlet header, and then unevenly distributes into the thirty fin channels according to the flow resistance of each fin channel. Air-flows across the heat transfer area along the air-side fin channels. The main geometric structure of the fins was described in the literature [27, 28].

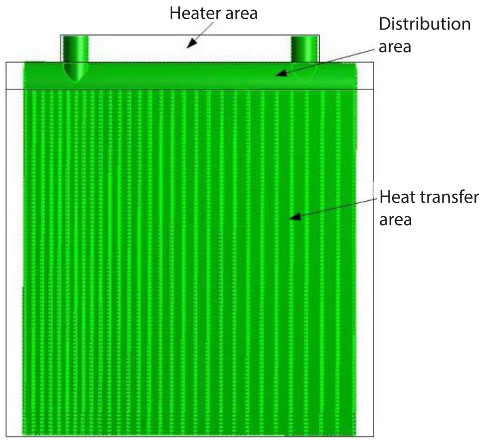

Figure 2. Geometric depiction of the non-equally PFHE

Simulation conditions and assumptions

In the numerical study of 3-D finned-plate heat exchanger, the CFD code FLUENT was used to simulate the flow fields inside the PFHE. On account of the limit by computing capacity, it is very hard to carry out the full-size numerical simulation, so the method based on porous media model becomes a common approach for numerical simulation of the heat exchanger. In the approach based on porous media model, the grid number and calculation cost are smaller than those in practical physical model. Especially in case of finned-plates, number of grids applied in the simulation based on porous media model is far less than the grid quantity in the practical physical model simulation, but the pressure drop obtained by the porous media model is almost equal to the result obtained from the practical physical model [15, 16]. Thus, we defined the offset fins in the channels as porous media. The effects of the offset fins on flow distribution and pressure drop of the PFHE can be obtained by setting viscous resistance and inertial resistance of that porous region. In this paper, a local fin model was simulated to develop the porous formulation for the fin channel for the first time. Based on the porous formulation, the thermodynamic characteristics of the full-size PFHE model was then studied by defining its fin channels as porous media.

Governing equations

Based on the aforementioned assumptions, a general governing equation used to describe the fluid-flow in the model was established:

$$\frac{\partial(\rho\phi)}{\partial t}+\mathrm{div}(\rho U\phi)=\mathrm{div}(\Gamma\,\mathrm{grad}\phi)+S \tag{1}$$

where ϕ is the general variable, Γ – the diffusion coefficient, U – the velocity vector, and S – the source term.

Porous media are modelled by adding a momentum source term to the general governing equation. The momentum source term impact the pressure gradient of the porous media area, and generate a pressure drop which is proportional to the square of velocity. The source term, S_i, which is composed of viscous loss term and inertial loss term, can be defined:

$$S_i=-\left(\sum_{j=1}^{3}\mathrm{D}_{ij}\mu v_j+\sum_{j=1}^{3}\mathrm{C}_{ij}\frac{1}{2}\rho|v|v_j\right) \tag{2}$$

where μ is the dynamic viscosity of the fluid, v_j – the face velocity for the j^{th} (x, y, or z) direction, $|v|$ – the magnitude of the velocity, $[D]$ and $[C]$ can been prescribed matrices. For simple homogeneous porous media, the source term can be further simplified:

$$S_i=-\left(\frac{\mu}{\alpha}v_i+\frac{1}{2}C_2\rho|v|v_j\right) \tag{3}$$

The first term on the right-hand side of eq. (3) takes into consideration the permeability of the porous medium, α, while the second term takes into consideration the inertial resistance factor, C_2. The matrix D, C is simplified as diagonal matrix and the diagonal coefficient is $1/\alpha$ and C_2, respectively, the other elements are zero.

The governing equations in primitive variables were discretized by the finite-volume method. To reduce numerical diffusion, a second-order upwind differential scheme was selected for the discretization of the momentum equations. The SIMPLER algorithm was adopted for the treatment of velocity-pressure coupling.

The basic assumptions and settings

For simplicity, the following assumptions are applied:

– Physical property variation of the fluids with temperature is neglected and the air is assumed to be ideal gas.

- The non-equally PFHE is operating under steady-state condition and both fluids are assumed to be stable.
- Heat transfer coefficients and the area distribution are assumed to be uniform and constant.
- The wall is considered as an ideal surface, which means there are no burrs, scarped edges or adhesive substances in the wall.

In addition, the fin channels in oil side and air side are assumed to be porous media area and the porous media parameters will be given in the section *Determining porous coefficients and porosuty*. The calculation domain in simulation process is the whole area shown in fig. 1. All of fin surfaces are fluid-solid coupling heat transfer and the temperature distribution can be iterative calculated by finite element software ANSYS FLUENT 13. The fluid of computational domain is assumed for the 3-D, turbulence, steady-state and no viscous dissipation. The pressure-velocity coupling is treated with SIMPLEC algorithm. Pressure terms in the governing equations are discretized by second-order central difference interpolation scheme. The second-order upwind scheme is considered to solve the velocity and temperature gradient terms and is also used for the interpolation if the terms are applied in turbulence closure models.To overcome the numerical divergence problem and get stable solutions, the under relaxation factor for the pressure, momentum, k and ε have been considered as 0.2, 0.5, and 0.5, respectively. The absolute convergence is understood when the residuals for all the governing equations reach a value of 10^{-6}.

Boundary conditions

The boundary conditions and governing equations together constitute a complete mathematical description of a physical problem. During the simulation, the velocity inlet boundary condition is employed in the inlet, and the inlet velocity value is determined according to the Reynolds number number under the calculation condition. The desired mass-flow rate and temperature values are assigned to the inlet of oil side and air side. Zero gauge pressure is assigned to the outlet of the oil side and the air side in order to obtain the relative pressure drop between inlet and outlet. No-slip boundary and impermeability conditions were enforced at walls. In this study, the inlet velocity was set to agree with experimental conditions. Boundary conditions are specified:

- *Inlet boundary conditions*: Due to the incompressible fluid on both sides, the initial velocity of fluid can be calculated according to the volume flow rate from the experimental data. So velocity inlet boundary conditions can be applied to the inlets of the oil side and air side, specified as following parameters:
- *Velocity specification method:* Magnitude, normal to boundary, can be chosen as the velocity magnitude [ms^{-1}] and the direction is perpendicular to the boundary.
- *Thermal/temperature*: according to the experimental data, the oil inlet temperature of 413 K.
- *Outlet boundary conditions*: The outlet boundary is the real pressure condition:

$$P = P_{\text{atm}}, \ \frac{\partial k}{\partial z} = \frac{\partial \varepsilon}{\partial z} = \frac{\partial T}{\partial z} = 0$$

Fluid outlet temperature is 377 K.

- *Wall boundary conditions*: The no-slip boundary condition and no-penetration at the wall boundary condition are defined for the numerical model. Top and bottom surface of the model is symmetric boundary and the wall material is defined as aluminum.

Accuracy and convergence

A careful grid size test with various inlet velocity was performed to ensure the accuracy of the previous discretization, where approximately 840000 and 12000000 grid elements were selected for the simulation of the local fin model and the full-size PFHE model, respectively. When the residual of each governing equation was reduced to 10^{-5} or smaller, the solution of each model was considered to converge to a stable level that was almost invariable.

Determining porous coefficients and porosity

Note that a simplified version of the momentum equation, relating the pressure drop to the source term, can be expressed:

$$\Delta P = -S_i \Delta n = \frac{\mu}{\alpha}\Delta n v_i + \frac{1}{2}C_2 \Delta n |v| v_i \tag{4}$$

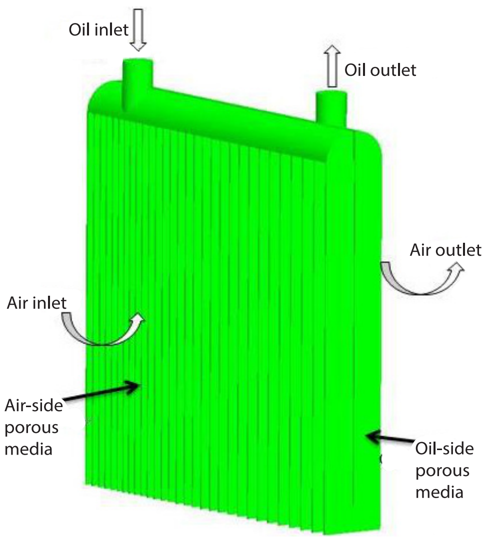

Figure 3. Porous media model of the non-equally PFHE

where Δn represents the porous media thickness. According to the eq. (4), the porous viscous resistance factor and inertial resistance factor of the defined the porous media region can be speculated if the relationship between pressure drop and velocity of fluid through the porous media region is obtained. The $C_1 = 1/\alpha$ is viscous resistance factor and C_2 is inertial resistance factor. In addition, the fin channels in the PFHE are assumed as isotropic which means the porous resistance coefficients in all three directions are the same.

A local CFD model of the offset fins was established to obtain the aforementioned relationships, as given in fig. 3. The meshing, boundary conditions and the simulation calculation method are all proposed in [27]. Here, these can be omitted. The comparison between the CFD and experimental results in terms of frication factor, f, as defined in eq. (5) demonstrated the validity of CFD method to get the hydrodynamic characteristics of the local fins model, as shown in tab. 1.

$$f = \frac{\Delta P D_\mathrm{h}}{2\rho v^2 L} \tag{5}$$

where Δp is the pressure drop of the local offset fins, L – fin array length, and D_h – the hydraulic diameter and defined:

– Oil side:

$$D_\mathrm{h,oil} = \frac{4A_c}{\dfrac{A}{l}} = \frac{2(s_2 + s_{2\_2})l_2 H_2}{(s_2 + s_{2\_2})l_2 + \dfrac{2H_2 l_2}{\sin\alpha} + \dfrac{2tH_2}{\sin\alpha}} \tag{6}$$

– Air side:

$$D_{h,air} = \frac{2s_1 H_1 l_1}{s_1 l_1 + H_1 l_1 + tH_1} \tag{7}$$

Table 1. Local fin simulation results on the both sides

Oil side		Air side	
Inlet velocity [ms^{-1}]	Pressure drop [Pa]	Inlet velocit [ms^{-1}]	Pressure drop [Pa]
0.6	647.38	6	52.73
0.7	801.8	7	64.48
0.8	967.81	8	78.58
0.9	1144.75	9	91.86

Based on the model, pressure drop of the offset fins under different fluid velocities were numerically calculated in both oil side and air side.

This validation model was computed in oil-side entrance velocity of 0.8 m/s and air-side inlet velocity of 9 m/s, respectively by using the commercial software FLUENT in ANSYS 13.0, and the temperature distribution of the model is described in fig. 4. The results show that the fins temperature is higher near the hot oil side than others. This phenomenon demonstrates that the cooling effect of air-side fins is more significant.

By using the least-square fit method, the correlations for pressure drop and fluid velocity are obtained.

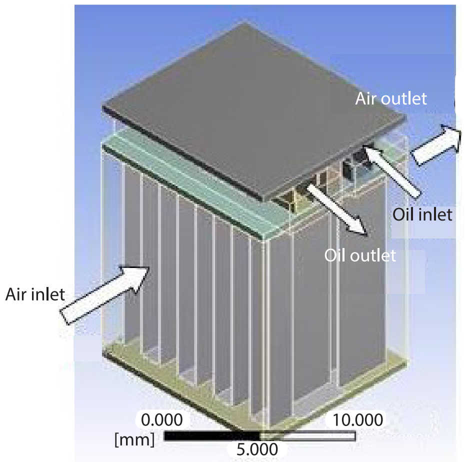

Figure 4. A local CFD model of the PFHE

– Oil side:

$$\Delta P = 640.9v^2 + 695.9v \tag{8}$$

– Air side:

$$\Delta P = 0.4743v^2 + 4.994v \tag{9}$$

Comparing eqs. (4) and (8), the oil- side porous coefficient can be obtained:

$$C_1 = \frac{1}{\alpha} = 1.33 \cdot 10^7, \ C_2 = 190$$

Similarly, the air- side porous coefficient can be obtained as:

$$C_1 = \frac{1}{\alpha} = 2.77 \cdot 10^7, \ C_2 = 104,16$$

Porosity refers to the ratio of the volume, V_p, available to flow in the tiny gap within porous medium and the total volume, V_b, of the porous media:

$$\varphi = \frac{V_p}{V_b} \tag{10}$$

Choosing a cycle period of the offset fin as the control volume in oil side:

$$\varphi_{\text{oil}} = 0.8948$$

Similarly, in air side:

$$\varphi_{\text{air}} = \frac{1845.5}{1845.5 + 155.86} = 0.9184$$

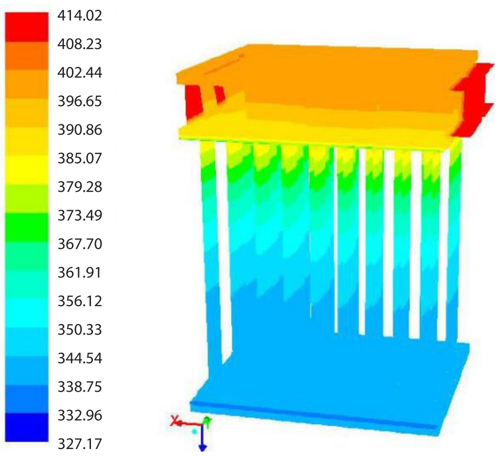

Figure 5. Temperature distribution of the local mode

Results and discussion

Validation of the porous media model

A full-size PFHE model with non-equally offset fins equivalent to actual equally geometry was built by adding the porous coefficients into the corresponding region, see fig. 1. Figure 5 shows temperature contour of the porous medium model and the thermodynamic characteristics comparisons are shown in tabs. 2 and 3. Table 2 shows the comparison of CFD results and experimental results in terms of the total heat transfer rate and tab. 3 shows the comparison of the total pressure drop. As seen in tabs. 2 and 3, the prediction from numerical simulation shows reasonably good agreement with the experimental data by the porous media approach.

Table 2. Comparison of total heat transfer rate between CFD and experimental data

Oil side				Air side			
Flow [m^3h^{-1}]	Experiment [kW]	Simulation [kW]	Error [%]	Flow [m^3h^{-1}]	Experiment [kW]	Simulation [kW]	Error [%]
4.480	56.79	53.64	–5.5	5106.3	54.45	53.52	–1.9
4.570	60.36	54.76	–9.3	5106.6	56.22	54.55	–3.0
4.800	71.25	75.74	6.3	5265.0	66.40	72.23	8.8
5.317	80.60	76.63	–4.9	5666.9	75.15	76.40	1.7
5.324	79.78	76.89	–3.6	5660.6	74.75	76.56	2.4
5.330	83.89	80.65	–3.9	5686.8	78.32	80.41	2.7
5.355	82.67	81.74	–1.1	5675.0	77.00	81.41	5.7
5.360	84.36	81.54	–3.4	5671.0	78.49	80.16	2.2
5.700	84.99	87.90	3.4	5623.1	79.76	87.66	9.9
6.420	86.40	89.16	3.2	5663.2	80.64	88.92	10.3
6.500	89.13	87.65	–1.7	5664.4	83.66	87.42	–4.5
6.508	90.04	87.98	–2.3	5659.4	84.18	87.75	4.3
6.585	90.24	89.58	–0.7	5696.6	84.90	89.33	5.2

Due to manufacturing and measurement errors as well as the numerical errors from the CFD model, the oil-side average deviations of the total heat transfer rate and the total pressure drop between the CFD and experimental results are about 2.2% and 4.3%, respectively. The air-side average deviations of the total heat transfer rate and the total pressure drop between the CFD and experimental results are about 3.7% and 3.2%, respectively. Hence, it can be concluded that the simulation is capable of closely predicting the thermodynamic characteristics of

Table 3. Comparison of the total pressure drop between CFD and experimental data

Oil side				Air side			
Flow [m^{3}h^{-1}]	Experiment [kPa]	Simulation [kPa]	Error [%]	Flow [m^{3}h^{-1}]	Experiment [kPa]	Simulation [kPa]	Error [%]
4.480	122.6	131.1	6.9	5106.3	0.5610	0.5419	–3.4
4.570	124.7	133.9	7.4	5106.6	0.5657	0.5420	–4.2
4.800	136.0	141.3	3.9	5265.0	0.5788	0.5668	–2.1
5.317	158.1	158.1	6.2	5666.9	0.6457	0.6321	–2.1
5.324	149.3	158.3	6.2	5660.6	0.6614	0.6331	–4.6
5.330	167.0	175.0	4.8	5686.8	0.6448	0.6354	–1.5
5.355	162.3	159.3	–0.4	5675.0	0.6514	0.6344	–2.6
5.360	161.4	159.4	–0.4	5671.0	0.6538	0.6338	–3.1
5.700	174.8	186.3	7.1	5623.1	0.6531	0.6328	–3.1
6.420	215.4	219.2	1.8	5663.2	0.6535	0.6317	–3.5
6.500	194.2	201.2	3.6	5664.4	0.6577	0.6321	–3.9
6.508	216.5	223.5	3.2	5659.4	0.6591	0.6317	–4.2
6.585	218.7	227.3	3.9	5696.6	0.6633	0.6370	–4.0

the PFHE. In this investigation, the deviation is evaluated through the overall average deviation parameter, which is defined:

– Average deviation:

$$\frac{1}{N}\left(\sum\frac{\phi_{\text{pred}}-\phi_{\text{exp}}}{\phi_{\text{exp}}}\right)\times 100\% \tag{11}$$

the position of import and export area for the heat exchanger head are different, resulting in the differences of mass-flow distribution at the export site and flow distribution, which can be evaluated through the overall standard deviation parameter STD:

$$STD=\sqrt{\frac{1}{n}\sum_{i=1}^{n}\left(\frac{\dot{m}_i}{\dot{m}_{\text{avg}}}-1\right)^2} \tag{12}$$

where $\dot{m}_i$ is the mass-flow rate in the i^{th} fin channel, $\dot{m}_{\text{avg}}$ – the average value of the mass-flow rate, and n – the number of fin channels.

Hydrodynamic distribution in the non-equally PFHE

The pressure and flow distribution inside the studied model are shown in fig. 6. Fluid velocity or kinetic energy decreases when the fluid-flows into the distribution area of the PFHE via the header. According to Bernoulli's principle, pressure or potential energy in that region will be increased as illustrated in fig. 6. Thus, fluid tends to go preferentially into the fin channels facing the inlet nozzle, and mass-flow rates of the fin channels corresponding to the inlet region of the header are greater than those of the other fin channels. As seen in fig. 6(b), vortexes are generated near the inlet tube due to a sudden enlargement of the cross-section. It was found that if these vortexes were intense enough, a depression at the entrance of some channels was created, which may eventually deteriorated flow distribution inside the PFHE.

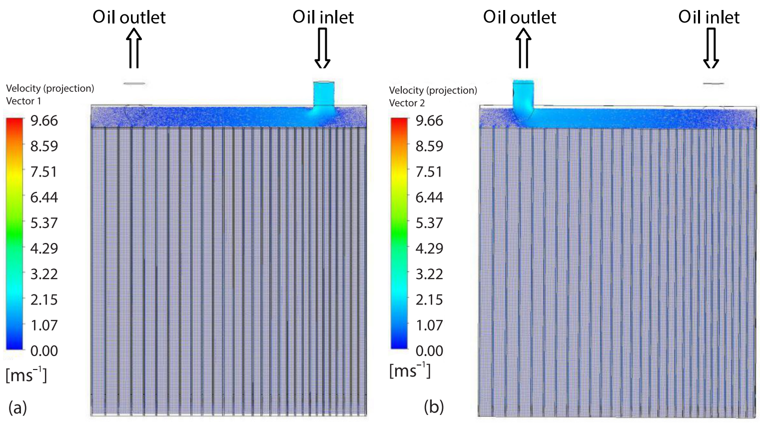

Figure 6. Velocity vectors of the porous medium model; (a) and (b)

Comparing of heater transfer resistance characteristics

Figure 7 shows comparing results of heater transfer resistance characteristics for the original model and the asymmetric model of the PFHE in terms of the pressure and heat transfer rate, respectively. Note that the proposed strategy can greatly improve heat transfer rate of the heat exchanger. As shown in figs. 7(a) and 7(b), when the air-side inlet velocity is 9 m/s, the total heat transfer rate is increased by 2.5-6.2% and the pressure drop remain basically constant or decreased slightly with the increase of oil flow velocity.

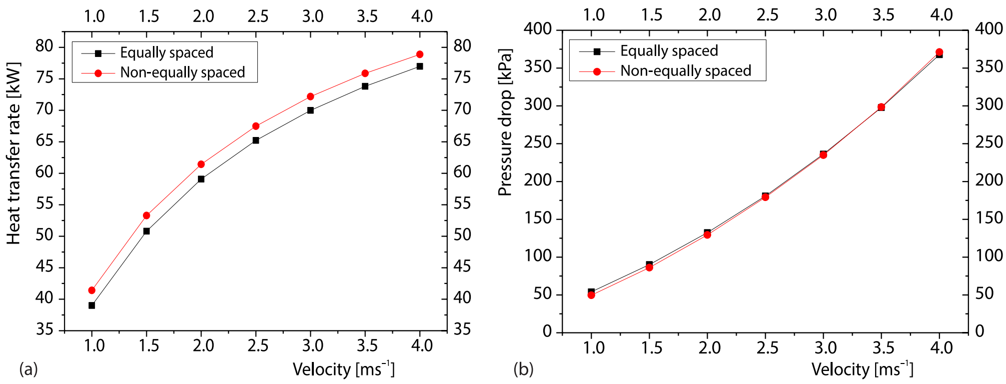

Figure 7. Comparison of numerical predictions of heat transfer rate and pressure drop under various inlet velocity; (a) velocity-heat transfer and (b) velocity-pressure drop

Conclusions

In order to investigate the thermodynamic characteristics of a full-size non-equally spaced PFHE, a full-size non-equally spaced numerical model was proposed by applying the porous media approach. The pore parameters as porous coefficients and porosity can be obtained by the local simulation results, and the model was verified by the experimental data. The numerical results show that the proposed strategy can greatly improve heat transfer rate of the heat exchanger. The total heat transfer rate is increased by 2.5-6.2% and the pressure drop remains basically constant or decreased slightly with the increased oil flow velocity, are as follows.

- The traditional full-size simulation model calculation is very hard to implement under the condition of current computer hardware for the PFHE studied in this article. By defining two side fins as porous media, the proposed model can be considered thermally equivalent to the actual geometry. By simulating the local fins model, the least-square fit method was used to obtain the correlation for pressure drop and fluid velocity, and then the porous coefficients of the porous media regions were derived. The porous media model makes it possible to simulate the full-size PFHE by considering the actual number of fins inside the PFHE.
- The numerical results reveal that pressure drop and the flow distribution of the PFHE are strongly related to the fluid dynamic viscosity. It was found that flow distribution of the PFHE would be more and more uniform by increasing the fluid dynamic viscosity, while leading to an increase in the pressure drop.
- Flow distribution in the PFHE is closely related to the inlet Reynolds number and pressure drop of the studied model. A correlation among flow distribution, pressure drop, and Reynolds number was derived. It was found that the increase of the fluid dynamic viscosity or the viscous resistance factor of porous media diminishes the effect of Reynolds number on flow distribution in the PFHE.

Acknowledgment

This work is supported by the Key Project of Natural Science Research in Universities of Anhui Province (Project No. KJ2019A0544). Fuyang Municipal Government-Fuyang Normal University Horizontal Cooperation Projects in 2017 (No. XDHXTD201709, XDHX201743).

References

[1] Lemouedda, A., *et al*., Optimizaton of the Angle of Attack of Delta-Winglet Vortex Generators in a Plate-fin-and-Tube Heat Exchanger, *Int. J. Heat Mass Tran*., *53* (2010), 23-24, pp. 5386-5399

[2] Song, K. W., *et al*., The Optimal Arrangement of Vortex Generators for Best Heat Transfer Enhancement in Flat-Tube-Fin Heat Exchanger, *Int. J. Therm. Sci*., *132* (2018), Oct., pp. 355-367

[3] Salviano, L. O., *et al*., Thermal-Hydraulic Performance Optimization of Inline and Staggered Fin-Tube Compact Heat Exchangers Applying Longitudinal Vortex Generators, *Appl. Therm. Eng*., *95* (2016), Feb., pp. 311-329

[4] Muhammad, A., *et al*., Enhancement of Thermal and Hydraulic Performance of Compact Finned-Tube Heat Exchanger Using Vortex Generators (VG): A Parametric Study, *Int. J. Therm. Sci*., *140* (2019), June, pp. 154-166

[5] Hemant, N., Tiwari, S., Thermal Performance Analysis of Fin-Tube Heat Exchanger with Staggered Tube Arrangement in Presence of Rectangular Winglet Pairs, *Int. J. Heat and Mass Tran*., *161* (2021), 106723

[6] Hemant, N., Tiwari, S., Effect of Rectangular Winglet Pair in Common Flow Down Configuration on Heat Transfer from an Isothermal Heated Plate, *Heat Tran. Eng*., *39* (2018), 20, pp. 1774-1789

[7] Anupam, S., *et al.,* Enhancement of Heat Transfer in a Fin-Tube Heat Exchanger Using Rectangular Winglet Type Vortex Generators, *Int. J. Heat and Mass Tran.*, *101* (2016), Oct., pp. 667-681

[8] Patankar, S. V., Spalding, D. B., *Heat Exchanger Design Theory Source Book*, McGraw-Hill, Book Company, New York, USA

[9] Sepideh, E., *et al*., Heat Transfer Enhancement in Shell and Tube Heat Exchangers Using Porous Media, *Heat Tran. Eng*., *36* (2015), 3, pp. 262-277

[10] Rao, B. P., Das, S. K., An Experimental Study on the Influence of Flow Maldistribution on the Pressure Drop Across a Plate Heat Exchanger, *Journal Fluids Eng.*, *126* (2004), 4, pp. 680-691

[11] Buyruk, E., Karabulut, K., Numerical Investigation into Heat Transfer for 3-D Plate Fin Heat Exchangers with Fins Placed Perpendicular to Flow, *Transactions of FAMENA*, *37* (2013), 2, pp. 87-102

[12] Buyruk, E., *et al*., The 3-D Numerical Investigation of Heat Transfer for Plate Fin Heat Exchangers, Heat Mass Trans., *49* (2013), 6, pp. 817-826

[13] Zhang, Q., Qin, S., *et al*., Simulation and Experimental Investigation of the Wavy Fin-and-Tube Intercooler, *Case Studies in Thermal Engineering*, *8* (2016), Sept., pp. 32-40

[14] Wang, W., *et al.*, Numerical Study on Hydrodynamic Characteristics of Plate-Fin Heat Exchanger Using Porous Media Approach, *Comp. and Chemical Eng*., *61* (2014), Feb., pp. 30-37
[15] Musto, M., *et al*., A Simplified Methodology to Simulate a Heat Exchanger in an Aircraft's Oil Cooler by Means of a Porous Media Model, *Appl. Therm. Eng*., *94* (2016), Feb., pp. 836-845
[16] Li, Z.-Z., *et al.*, An Approach Based on the Porous Media Model for Numerical Simulation of 3-D Finned-tubes Heat Exchanger, *Int. J. Heat Mass Tran*., *173* (2021), 121226
[17] Sahin, B., et al., Optimum Design Parameters of a Heat Exchanger, *Appl. Energy*, *82* (2005), 1, pp. 90-106
[18] Muhammad, M. A. B., *et al.*, The CFD Applications in Various Heat Exchangers Design: A Review, Appl. Therm. Eng., *32* (2012), Jan., pp. 1-12
[19] Zhang, Z., *et al*., Experimental Invsetigation of Distributor Configuration on Flow Maldistribution in Plate-Fin Heat Exchangers, *Applied Thermal Engineering*, *25* (2015), 85, pp.111-23
[20] Manglik, R. M. ,Bergles, A. E., *The Thermal-Hydraulic Design of the Rectangular Offset-Strip-Fin Compact Heat Exchanger*, (Eds. Shahet, R. K., *et al*.), Hemisphere, New York, USA, 1990, pp. 123-149
[21] Wahiba, Y., *et al*., The 3-D Study of the Effect of Inlet Air-Flow Maldistribution on Plate-Fin-Tube Heat Exchanger Design and Thermal-Hydraulic Performance, *Int. J. Heat and Mass Trans*., *101* (2016), Oct., pp. 527-541.
[22] Buyruk, E., Karabulut, K., Research of Heat Transfer Augmentation in Plate Fin Heat Exchangers Having Different Fin Types, *Journal of Engineering Thermophysics*, *29* (2020), 2, pp. 316-330
[23] Muller-Menzel, T., Hecht, T., Plate-Fin Heat Exchanger Performance Reduction in Special Two-Phase Flow Conditions, *Cryogenics*, *35* (1995), 5, pp. 297-301
[24] Hajabdollahi, H., Seifoori, S., Effect of Flow Maldistribution in the Optimal Design of a Cross-Flow Heat Exchanger, *Int. J. Therm. Sci.*, *109* (2016), Nov., pp. 242-252
[25] Blecich, P.. Experimental Investigation of the Effects of Air-Flow Non-Uniformity on Performance of a Fin-and-Tube Heat Exchanger, *International Journal of Refrigeration*, *59* (2015), Nov., pp. 65-74
[26] Ranganayakulu, C., Seetharamu, K. N., The Combined Effects of Wall Longitudinal Heat Conduction and Inlet Fluid-Flow Maldistribution in Crossflow Plate-Fin Heat Exchangers, *Heat Mass Trans*., *36* (2000), 30, pp. 247-256
[27] Du, J., Experimental Study and Numerical Simulation of Flow and Heat Transfer Performance on an Offset Plate-Fin Heat Exchanger, *Heat and Mass Transfer*, *52* (2015), Oct., pp. 1791-1806
[28] Du, J., *et al*., Correlations and Optimization of a Heat Exchanger with Offset Fins by Genetic Algorithm Combining Orthogonal Design, *Appl. Therm. Eng*., *107* (2016), Aug., pp. 1091-1103

Paper submitted: December 27, 2021
Paper revised: January 29, 2022
Paper accepted: February 28, 2022